

Article

Relative Transport Behavior of *Escherichia coli* O157:H7 and *Salmonella enterica* Serovar Pullorum in Packed Bed Column Systems: Influence of Solution Chemistry and Cell Concentration

B. Z. Haznedaroglu, H. N. Kim, S. A. Bradford, and S. L. Walker

Environ. Sci. Technol., **2009**, 43 (6), 1838-1844 • DOI: 10.1021/es802531k • Publication Date (Web): 06 February 2009

Downloaded from <http://pubs.acs.org> on March 16, 2009

More About This Article

Additional resources and features associated with this article are available within the HTML version:

- Supporting Information
- Access to high resolution figures
- Links to articles and content related to this article
- Copyright permission to reproduce figures and/or text from this article

[View the Full Text HTML](#)

Relative Transport Behavior of *Escherichia coli* O157:H7 and *Salmonella enterica* Serovar Pullorum in Packed Bed Column Systems: Influence of Solution Chemistry and Cell Concentration

B. Z. HAZNEDAROGLU,[†] H. N. KIM,[†]
S. A. BRADFORD,[‡] AND S. L. WALKER^{*†}

Department of Chemical & Environmental Engineering,
University of California, Riverside, California 92521, and
Salinity Laboratory, Agricultural Research Service, United
States Department of Agriculture, Riverside, California 92521

Received October 13, 2008. Revised manuscript received
December 11, 2008. Accepted December 16, 2008.

The influence of solution chemistry and cell concentration on bacterial transport has been examined using *Salmonella pullorum* SA1685 and *Escherichia coli* O157:H7. A column was employed to determine the transport behavior and deposition kinetics with aquifer sand over a range of ionic strengths and cell concentrations. O157:H7 was found to be more adhesive than SA1685, with calculated deposition rate coefficients higher than those of SA1685. Comprehensive cell surface characterization techniques including size, surface charge density, extracellular polymeric substance content, electrophoretic mobility, and hydrophobicity analyses were conducted to explain observed transport trends. The pathogens' size and hydrophobicity were not significantly different, whereas they varied in acidity, for which O157:H7 had 19 times higher surface charge density than SA1685. Electrophoretic mobilities, in general agreement with titration analysis and column experiments, revealed SA1685 to be more negative than O157:H7. This combination of column and characterization experiments indicates that SA1685 can be transported to a greater extent than O157:H7 in groundwater environments. This study is the first comprehensive work comparing the transport behavior of two important pathogens in aquifer systems.

Introduction

In the United States there are 238 000 animal feeding operations producing 317 million tonnes of liquid and solid manure annually (1), which contains a variety of pathogenic microorganisms (2). For example, the shedding rate of *Salmonella* in poultry may be as high as 10⁵ to 10⁶ CFUs/g (3), and up to 10² to 10⁴ CFUs/g of *Escherichia coli* O157:H7 in calf manure (4). Precipitation and surface water flow can cause pathogens to leach from manure to flowing water (5). Concentrations of *E. coli* O157:H7 from land-applied animal manure can reach levels of 10⁷ CFUs/mL within 3 hours in silty clay and sandy loam soil (6). Hence, improperly treated

manure and manure-contaminated water can pose a risk to human and animal health when used as a source for irrigation or groundwater recharge (1, 7).

Recent studies have shown that half of all the U.S. drinking water wells tested had fecal pollution, causing an estimated 750 000 to 5.9 million illnesses per year (8). Drinking water outbreaks in the U.S. have primarily been associated with inadequately disinfected groundwater and distribution system contamination, with a significant number of these outbreaks being caused by *E. coli* O157:H7 and *Salmonella* spp (9). *E. coli* O157:H7 causes an estimated 73 000 cases of infection and 60 deaths in the U.S. annually (10). Waterborne outbreaks associated with various subspecies of *Salmonella* have been traced to contaminated wells and water storage and have been estimated to cause 1 412 498 cases of acute gastroenteritis illnesses in the United States annually (11).

Salmonella pullorum is an especially serious avian pathogen causing "pullorum disease" in infected chickens and turkeys (12). Usually newly hatched birds are the primary victims (13), although there are reports of infection to other animals (14). *S. pullorum* is also of interest due to increasing development of antibiotic resistance among zoonotic pathogens (15).

To address bacterial pollution in groundwater environments and to prevent the spread of infectious diseases to humans via this means of transport, there is an immediate need for a comprehensive understanding of the fate and transport of pathogens of concern. Therefore, this study was designed to investigate the transport behavior of *S. pullorum* and *E. coli* O157:H7 under a variety of solution chemistry conditions and cell concentrations, consistent with the variability of natural environments. Extensive cell surface characteristics were compared to provide an explanation for the calculated differences in pathogen travel distances under test conditions.

Materials and Methods

Bacterial Cell Selection and Preparation. *S. pullorum* strain SA1685 obtained from the Salmonella Genetic Stock Centre, University of Calgary, Canada, is a nonmotile, nonflagellated avian pathogen originally isolated from an infected turkey. *E. coli* O157:H7 strain p72 was also nonflagellated and nonmotile under the utilized cell growth conditions, and was obtained from the USDA (Pina Fratamico, USDA-ARS-ERRC, Wyndmoor, PA). Details on bacterial preparation methods are presented in the Supporting Information.

Bacterial Cell Characterization. Viability tests were conducted on SA1685 and O157:H7 using the Live/Dead BacLight kit (L-7012, Molecular Probes, Eugene, OR) in 10 mM KCl solution. Direct counting of the stained cells was done using an inverted microscope (IX70, Olympus, Japan) and the appropriate fluorescence filter (Chroma Technology Corp., Brattleboro, VT).

To measure the dimensions of SA1685 and O157:H7, phase contrast images were taken using an inverted microscope (IX70, Olympus) and a camera (Retiga 1300, Qimaging, Canada) at ~10⁸ cells/mL in 10 mM KCl. Images of cells ($n > 60$) were processed (SimplePCI, Precision Instruments Inc., Minneapolis, MN), and individual cell lengths and widths were determined. Measured values were used to calculate the effective cell radius and corresponding bacterial surface area.

Hydrophobicity analysis of the cells was done using the microbial adhesion to hydrocarbons (MATH) test (16). Briefly, the partitioning of cells was measured between a hydrocarbon (*n*-dodecane, laboratory grade, Fisher Scientific, Fairlawn,

* Corresponding author phone: (951) 827-6094; fax: (951) 827-5696; e-mail: swalker@engr.ucr.edu.

[†] University of California.

[‡] United States Department of Agriculture.

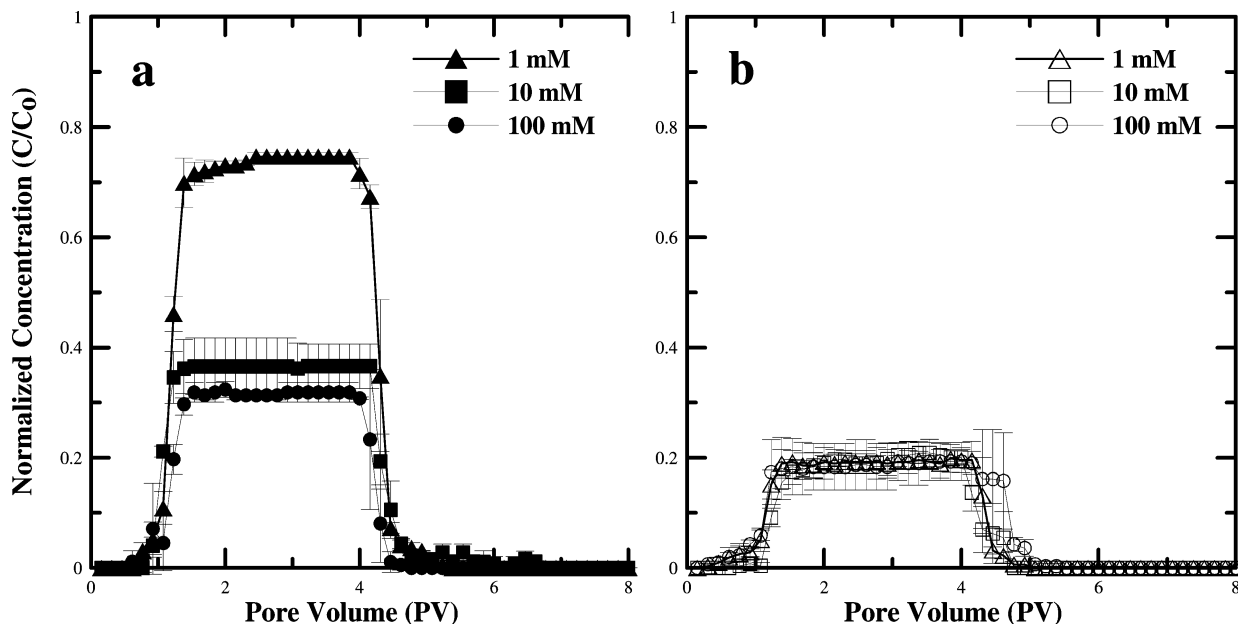


FIGURE 1. BTCs of SA1685 (a) and O157:H7 (b) tested at 1, 10, and 100 mM IS ($C_0 = 10^7$ cells/mL). Error bars indicate the average of three runs.

NJ) and electrolyte solution (10 mM KCl) as the percentage of total cells partitioned into the hydrocarbon from the aqueous phase.

Potentiometric titrations of cells were conducted to determine the relative acidity and charge density of the bacterial surfaces. An autotitrator (798 MPT Titrino, Metrohm, Switzerland) was used to determine the amount of base consumed by suspended cells during titration between pH 4 and pH 10. Bacterial suspensions with concentrations of $(3-5.3) \times 10^8$ cells/mL in 10 mM KCl were titrated by 0.3 N NaOH. The resulting acidity and corresponding surface charge density were calculated (17, 18).

The extracellular polymeric substance (EPS) composition, specifically the total protein and sugar content, was analyzed on the basis of an established extraction method (19). The pellet of harvested bacterial cells was suspended in formaldehyde–NaCl solution followed by various centrifugation steps and final exposure to ethanol–KCl solution. The analysis of protein was performed using the Lowry method (20) with bovine serum albumin (BSA; 20 mg/mL) (Fisher Scientific) as the standard and measured spectroscopically (BioSpec-mini, Shimadzu, Kyoto, Japan) at a wavelength of 500 nm. The analysis of total sugars was performed using the phenol–sulfuric acid method described previously (21). Xanthan gum (practical grade, Fisher Scientific) was used as the standard, and samples were measured spectroscopically at 480 nm (BioSpec-mini, Shimadzu).

Electrokinetic Properties and DLVO Calculations. Details regarding measurement of bacterial electrophoretic mobility and total interaction energy calculations are given in the Supporting Information.

Column Experiments. Chromaflex chromatography columns (Kontes Glass Co., Vineland, NJ) 2.5 cm in diameter and 60 cm long were wet packed using autoclaved quartz sand (710 μm). Further details are given in the Supporting Information.

Deposition Profile and Extent of Kinetics. To determine the deposition profile of bacteria across the length of the column, sand was excavated after the experiment (27). The total percentage (M_{total}) of cells recovered was determined from the sum of the percentages of cells recovered from the column effluent (M_{eff}) and the aquifer sand (M_{sand}) by following a protocol described previously (62, 63).

The bacterial deposition rate coefficient, k_d , was determined by (22,26,28)

$$k_d = -\frac{U}{\varepsilon L} \ln\left[\frac{C}{C_0}\right] \quad (1)$$

where C/C_0 is the normalized concentration exiting the column, U is the superficial velocity, ε is the porosity, and L is the length of the packed bed. The average value of C/C_0 was obtained between 1.8 and 2.0 pore volumes (PV), which represents “clean-bed” conditions (29). Approximate travel distances of SA1685 and O157:H7 were estimated from measured values of k_d . Details of the deposition profile, mass balance, and travel distance equations are given in the Supporting Information.

Results

Bacterial Transport. Results of transport experiments are presented in terms of the influence of the solution chemistry and injection concentrations (C_0). Breakthrough curves (BTCs) of SA1685 and O157:H7 showing the effects of the solution chemistry are presented in Figure 1 when $C_0 = 10^7$ cells/mL. As observed in Figure 1a, SA1685 retention in the column increased with the ionic strength (IS), approximately 27%, 64%, and 69% at 1, 10, and 100 mM, respectively. Retention of O157:H7 was independent of the IS, and approximately 80% of the bacteria were retained as shown in Figure 1b.

The effect of the cell concentration (10 mM KCl) is depicted in Figure 2. Cell retention was nearly identical when C_0 was 5×10^6 and 10^7 cells/mL, with an average retention of 63% for SA1685 (Figure 2a) and 80% for O157:H7 (Figure 2b). At $C_0 = 10^8$ cells/mL, the values of C/C_0 in BTCs increased $\sim 20\%$ between 1 and 4 PV for both cell types.

Figure 3 presents k_d as a function of the IS and C_0 . As expected, the k_d values follow the same trend as cell retention. Namely, when 10^7 cells/mL was injected, the k_d values were virtually identical at all ISs for O157:H7, whereas the k_d values increased with the IS for SA1685. The k_d values of both SA1685 and O157:H7 in 10 mM KCl were essentially independent of C_0 at 5×10^6 and 10^7 cells/mL, but slightly decreased at $C_0 = 10^8$ cells/mL.

Deposition Profiles. Deposition profiles were determined following completion of transport experiments and are

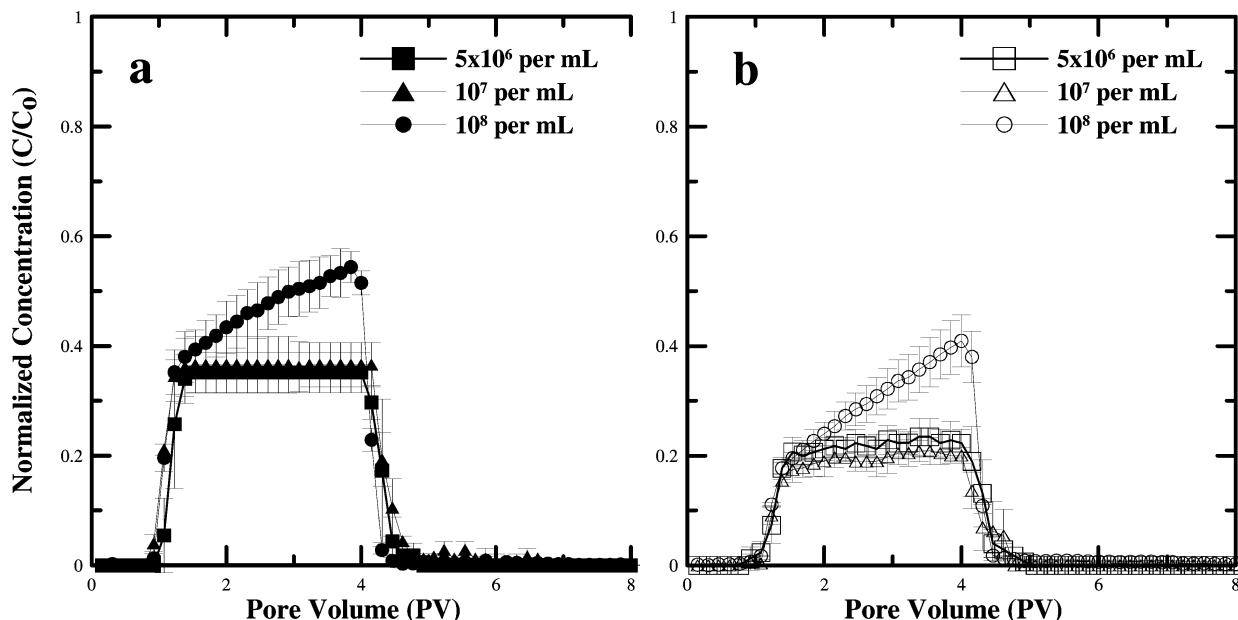


FIGURE 2. BTCs of SA1685 (a) and O157:H7 (b) tested at different C_0 values (10 mM KCl). Error bars indicate the average of three runs.

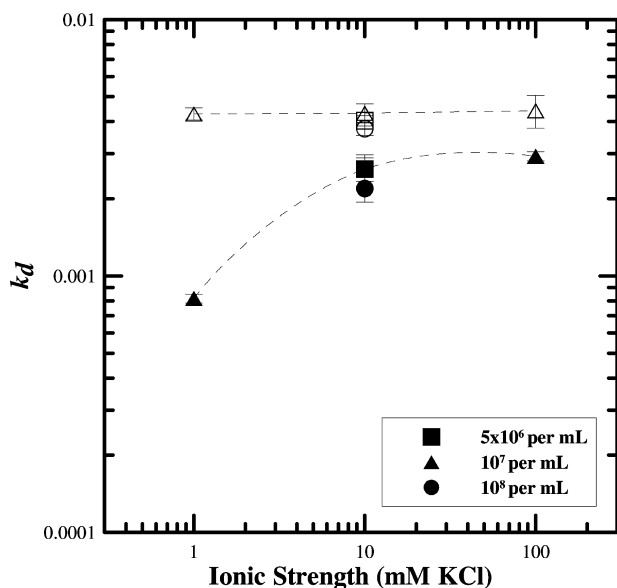


FIGURE 3. Deposition rate coefficient (k_d) versus IS for SA1685 (closed shapes) and O157:H7 (open shapes) injected at 5×10^6 cells/mL (squares), 10^7 cells/mL (triangles), and 10^8 cells/mL (circles). The dashed lines are drawn to provide guides to the eye to indicate trends in changing k_d . Error bars indicate 1 standard deviation.

reported in the Supporting Information. Figure S1 shows deposition profiles for SA1685 (Figure S1a,b) and O157:H7 (Figure S1c,d) with respect to the influence of the solution chemistry and C_0 . When 10^7 cells/mL of SA1685 was injected, the bacterial concentration retained in the column normalized by the mass of sand increased with the IS (Figure S1a), similar to the observed BTCs. In the case of O157:H7 there were no significant changes observed with the IS (Figure S1c), like the observed BTCs. In terms of C_0 the number of SA1685 cells retained in the column was similar at 5×10^6 and 10^7 cells/mL; however, a decrease was observed at $C_0 = 10^8$ cells/mL (Figure S1b). The amounts of O157:H7 retained in the column at all C_0 values were similar (Figure S1d), and no trend with the injection concentration was observed.

Table S1 indicates that a reasonable mass balance was achieved in the column experiments (78–127%).

Travel Distances. On the basis of the experimental results, travel distances were calculated at which 99.9% of the cells would be removed (60–62). SA1685 was transported further than O157:H7 at comparable IS and C_0 conditions (Figure S2, Supporting Information). The longest travel distance calculated for SA1685 was 11.8 m at 1 mM and a C_0 of 10^7 cells/mL. O157:H7 travel distances were similar under all conditions, with 3.7 m as the longest travel distance at 10 mM and $C_0 = 10^8$ cells/mL. It should be mentioned that these are conservative estimates of travel distance, as k_d was assumed independent of concentration whereas k_d was slightly greater at lower injection concentrations (Figure 3).

Electrokinetic Properties and DLVO Profiles. The electrophoretic mobilities of SA1685 and O157:H7 were negatively charged under all conditions (Table 1), with SA1685 being more negative than O157:H7. Increased IS caused a reduction in mobility for SA1685 due to compression of the electric double layer (30). In contrast, differences in O157:H7 mobility with the IS were not statistically significant.

Measured ζ potentials of sand particles are reported in Table 2. These values were used in lieu of surface potentials to calculate the interaction energy existing between cells and sand particles using DLVO theory (25). DLVO theory predicts favorable attachment conditions for O157:H7 at 10 and 100 mM and for SA1685 at 100 mM. Conversely, unfavorable attachment conditions are predicted for these bacteria at the other IS conditions (1 mM for O157:H7, 1 and 10 mM for SA1685). At 1 mM, cells experience energy barriers greater than $3.16 kT$ to attachment to the collector surface. At 10 mM, an energy barrier of $9.87 kT$ exists between SA1685 and sand. Additionally, the predicted secondary minimum depths for SA1685 and O157:H7 were negligible at all ISs.

Bacterial Surface Characteristics. Cell characteristics of SA1685 and O157:H7 are presented in Table 1. Size measurements showed no significant difference between the two pathogens. MATH test results indicate both were similarly hydrophobic (16.74–26.72%). Potentiometric titration revealed that O157:H7 was more acidic than SA1685, with more dissociable functional groups and greater charge density. Measured values of acidity were 0.47×10^{-5} , 0.19×10^{-5} , and

TABLE 1. Key Cell Characteristics of SA1685 and O157:H7

strain	IS (mM KCl)	radius ^a (μm)	acidity ^b	surface charge density ^c	MATH ^d (%)	sugar concn ^e (μg/mL)	protein concn ^f (μg/mL)	mobility [(μm/s)/(V/cm)]	ζ potential (mV)	viability ^g (%)
			(mequiv/10 ⁸ cells)	(μC/cm ²)						
SA1685	1		0.47 × 10 ⁻⁵	180	26.19 ± 2.20			-0.87 ± 0.09	-11.11 ± 1.16	95 ± 1.21
	10	0.455 ± 0.08	0.19 × 10 ⁻⁵	75	17.74 ± 5.05	6.75 ± 0.84	289.30 ± 24.73	-0.65 ± 0.04	-8.23 ± 0.70	92 ± 2.34
	100		0.18 × 10 ⁻⁵	68	26.45 ± 9.96			-0.59 ± 0.21	-7.54 ± 2.71	91 ± 3.23
O157:H7	1		1.49 × 10 ⁻⁵	512	26.72 ± 9.33			-0.18 ± 0.28	-2.23 ± 3.57	94 ± 2.27
	10	0.480 ± 0.06	8.48 × 10 ⁻⁵	2840	18.83 ± 1.92	1.75 ± 0.16	139.61 ± 12.71	-0.14 ± 0.13	-1.84 ± 1.62	91 ± 1.92
	100		3.0 × 10 ⁻⁵	1027	16.74 ± 6.70			-0.12 ± 0.16	-1.60 ± 2.04	93 ± 0.83

^a Value for the equivalent spherical radius calculated from the measured length and width of individual cells. ^b Acidity determined from the amount of NaOH consumed during titration between pH 4 and pH 10. ^c Density of charged functional groups across the cell surface. The value determined from the measured acidity and accounting for the exposed surface area of the cells (calculated for a spherical cell) and Faraday's constant is 96 485 C/mol. ^d MATH indicates the relative hydrophobicity of the cell as the percentage of cells partitioned in dodecane versus electrolyte. ^e Based on the phenol-sulfuric acid method with xanthan gum as the standard at 10⁸ cells/mL. ^f Based on the Lowry method with BSA as the standard at 10⁸ cells/mL. ^g Percentage of the cell population viable based on the Live/Dead BacLight kit. Values are averages of the measured viability across the range of ISs utilized in transport experiments.

TABLE 2. ζ Potential of Sand Particles, Energy Barrier Heights, and Secondary Energy Minimum Depths As a Function of the IS As Calculated by DLVO Theory^a for SA1685 and O157:H7

strain	IS (mM KCl)	sand particle	cell-sand interactions	
		ζ potential ^b (mV)	primary max (kT)	secondary min (kT)
SA1685	1	-26.02 ± 1.48	94.83	NB ^c
	10	-15.30 ± 0.73	9.87	NB
	100	-1.81 ± 4.7	NB	NB
O157:H7	1	-26.02 ± 1.48	3.16	NB
	10	-15.30 ± 0.73	NB	NB
	100	-1.81 ± 4.7	NB	NB

^a Calculations done assuming a Hamaker constant of 6.5 × 10⁻²¹ J (60) and using the bacterial sizes reported in Table 1. ^b ζ potential values were calculated from the streaming potentials (23, 24). ^c NB denotes no energy barrier.

0.18 × 10⁻⁵ mequiv/10⁸ cells for SA1685 at 1, 10, and 100 mM, respectively. O157:H7 acidity values were measured as 1.49 × 10⁻⁵, 8.48 × 10⁻⁵, and 3 × 10⁻⁵ at 1, 10, and 100 mM, respectively. From these values, the surface charge densities were calculated (18) as 180, 75, and 68 μC/cm² for SA1685 and 512, 2840, and 1027 μC/cm² for O157:H7 at 1, 10, and 100 mM, respectively. EPS analysis revealed SA1685 had almost 4 times more sugar content than O157:H7, with a similar trend for protein. Viability test results revealed greater than 90% viability at all conditions.

Discussion

Effect of the IS. Electrophoretic mobilities indicate SA1685 to be more negatively charged than O157:H7. Conversely, titration results indicate higher acidity and surface charge density for SA1685 compared with O157:H7. This apparent discrepancy in cell charge results can be explained by differences in the measurement techniques. Electrophoretic mobility reflects the net surface charge, whereas titration captures the density of dissociable functional groups on the membrane surface and within the macromolecular (EPS) complex. Furthermore, titration results may be sensitive to the cell size and interspecies variation. Hence, electrophoretic mobility provides a better indication of cell-cell and cell-quartz interactions than titration results. Indeed O157:H7 had a higher (less negative) electrophoretic mobility (Table 1) and greater cell retention than SA1685 (Figure 1) at a given

IS, a result consistent with DLVO theory. The deposition rate coefficients were also constantly higher for O157:H7 than SA1685 (Figure 3).

DLVO theory was also able to qualitatively explain the transport and adhesion trends for SA1685. As observed in Figure 1a, SA1685 retention in the column increased with the IS. This was an expected trend due to double-layer compression occurring with increasing IS. Electrophoretic mobility and ζ potential trends also confirmed this with decreased values with increasing IS. As SA1685 experienced the highest primary energy barrier that must be overcome for attachment at 1 mM, retention in the column was much less at 1 mM than at 10 and 100 mM conditions where SA1685 experienced a small energy barrier (9.87 kT) and no barrier, respectively. SA1685 therefore achieved its longest transport distance at 1 mM when the pathogen had the highest ζ potential.

Retention of O157:H7 was independent of the IS (Figure 1b). It was observed that the *k_a* values of O157:H7 were similar at all conditions, with ~20% of the pathogen breaking through. This is attributed to the surface being relatively insensitive to the solution chemistry as observed by the electrophoretic mobility and hydrophobicity values overlapping at 1, 10, and 100 mM. Travel distances for O157:H7 were therefore virtually identical and independent of the IS for 10⁷ cells/mL.

It is interesting to note that DLVO theory predicts favorable (10 and 100 mM for O157:H7 and 100 mM for SA1685) and/or near-favorable conditions (a minor energy barrier of 3.16 kT occurred at 1 mM for O157:H7, hardly more than Brownian motion could overcome (39) occurred for some of the experiments. Classic filtration theory would predict very limited transport under such favorable conditions. The observed significant transport behavior (Figures 1–3 and S1 and S2, Supporting Information) and the reasonable mass balance results (Table S1) however suggest the cells were not irreversibly retained in the primary minimum. Recent literature indicates that steric stabilization of macromolecules on the surface of microorganisms may hinder attachment in the primary minimum (54) and that hydrodynamic forces may remove weakly associated cells from collector surfaces (55).

Effect of the Cell Concentration. *C₀* values of 5 × 10⁶ and 10⁷ cells/mL did not change retention values for either pathogen; however, at 10⁸ cells/mL, BTCs displayed increasing *C/C₀* values for both O157:H7 and SA1685 (Figure 2). This trend has been explained in the literature by “blocking” (31–35), simultaneous bacterial deposition and release

(36–38), or colloid/microbial collisions and their effect on the filling of small pore spaces that are associated with enhanced retention (56). Blocking implies a limited number of favorable attachment sites and that deposited cells provide fewer favorable surfaces for subsequent cell attachment. Higher concentrations are expected to “block” favorable attachment sites more rapidly than lower concentrations and therefore exhibit less of a time dependency. This hypothesis is not consistent with the time-dependent shape of the BTC at the highest C_0 value shown in Figure 2. Furthermore, simultaneous cell deposition and release implies a high release rate, yet significant concentration tailing that was not observed in the BTCs. The latter mechanism—cell–cell collisions—seems most plausible. These collisions, which increase with concentration, may hinder retention by knocking weakly associated cells off the solid surface. This hypothesis is consistent with the observation that 10^7 cells/mL of either pathogen resulted in increased retention as compared to 10^8 cells/mL. The time dependency of the filling of the small pore spaces can also logically be expected to be a function of the cell concentration, due to plugging of small pore spaces at higher concentrations. In this study, the no time dependency of the rising portion of the BTC was observed when C_0 was less than 10^8 cells/mL, whereas when C_0 was greater than 10^8 cells/mL a time dependency in the BTC was observed, presumably due to filling of the smallest pore spaces.

Deposition Profiles. Deposition profiles for SA1685 (Figure S1a, Supporting Information) showed that the number of bacteria retained in the column increased with the IS. The influence of concentration was also confirmed with deposition profiles (Figure S1b) where bacteria numbers retained were lower at 10^8 cell/mL than in the 5×10^6 and 10^7 cells/mL cases. Deposition profiles for O157:H7 were similar at all tested IS and C_0 conditions.

Deposition profiles for many types of colloids (i.e., viruses and bacteria) have been reported to follow hyperexponential profile distributions, implying a decreasing rate of deposition with increasing travel distance (40–49). However, both SA1685 and O157:H7 showed a tendency to be retained in lower portions of the column, from a dimensionless depth of 0.5–1 (Figure S1, Supporting Information). Similar trends have been reported in the literature by Tong (50) and Bradford (27). Possible mechanisms to explain observed nonexponential deposition behavior may include time-dependent deposition (32, 51, 52) or particle detachment, both of which are implicated by the concentration-dependent trends discussed already (53). There are other explanations for nonexponential deposition profiles such as physical factors not included in filtration theory including “straining”, referred to as retention of bacterial cells in smaller pores and at grain–grain junctions (27, 29, 44, 58), surface roughness (47, 54), hydrodynamic drag (57, 59), and cell aggregation (27). Others have related the nonexponential behavior to heterogeneity within the bacterial suspension or population (50, 53), which produces a distribution of cells that interact with each other or the sand. In addition to these, hydrodynamic forces during the elution step might also displace cells and push them toward the lower regions of the column. This may be contributing, considering the column was flushed with 5 PV of electrolyte before column excavation at a high Darcy water velocity of 0.05 cm/s. The observed deposition trends are most likely a combination of these aforementioned phenomena.

Concluding Remarks and Implications. Relative transport trends of SA1685 and O157:H7 were investigated with a focus on the influence of the solution chemistry and cell injection concentration. Both experimental results and theoretical calculations were employed to predict these two important pathogens’ interactions and transport behavior in representative groundwater conditions. Cell surface

characterization experiments were conducted along with classical DLVO theoretical calculations.

Electrophoretic mobility analysis showed that SA1685 was more negative than O157:H7. Column experiment results were consistent with these observations as O157:H7 was retained more than SA1685. Interestingly, at higher injection concentration (10^8 cells/mL), both cell types showed increasing C/C_0 values and time dependency in the rising portion of the BTC. Travel distance calculations concluded that both pathogens can move long distances under possible groundwater conditions in terms of flow velocities, cell concentrations, and ISs. These calculations are based upon k_d values as determined for aquifer sand which are highly unfavorable and where maximum transport is anticipated. Top distances calculated were 3.7 m for O157:H7 and 11.8 m for SA1685 for viable cells within a period of a day, even when a 3 log removal was achieved.

This study shows that outbreak-causing pathogens such as SA1685 and O157:H7 may follow complex transport behavior in groundwater conditions, more so than straightforward trends of nonpathogenic species (35, 48), indicating additional mechanisms may be involved in their fate. In addition, other factors such as steric stabilization of cell surface macromolecules, cell collisions and interactions, cell heterogeneity, hydrodynamic drag forces, and considerations of pore structure will likely have to be considered to predict the fate of such pathogens. Additionally, relatively low and high cell concentrations may lead to considerable travel distances and pose water quality hazards. This study documents the first comparative transport behavior of *Salmonella pullorum* and *E. coli* O157:H7 in a wide range of potential groundwater conditions.

Acknowledgments

We acknowledge funding from the USDA HSI CSREES and the National Water Research Institute. We also acknowledge the contribution of an undergraduate student, Yasmine Salas, from Riverside Community College, also supported by the USDA grant.

Supporting Information Available

Further information on methods for bacterial and porous medium preparation, electrokinetic property determination, DLVO calculations, column experiments, determination of the deposition profile and kinetics, and travel distance calculations, mass balance table, and deposition profile and travel distance graphs. This information is available free of charge via the Internet at <http://pubs.acs.org>.

Literature Cited

- (1) Browner, C. M.; Fox, J. C.; Frace, S. E.; Anderson, D. F.; Goodwin, J.; Shriner, P. H. *Development Document for the Proposed Revisions to the National Pollutant Discharge Elimination System Regulation and the Effluent Guidelines for Concentrated Animal Feeding Operations*; Engineering and Analysis Division, Office of Science and Technology, U.S. Environmental Protection Agency: Washington, DC, 2001.
- (2) Gerpa, C. P.; Smith, J. E. Sources of pathogenic microorganisms and their fate during land application of wastes. *J. Environ. Qual.* **2005**, *34*, 42–48.
- (3) Griffint, P. M.; Bell, B. P.; Cieslak, P. R.; Tuttle, J.; Barrett, T. J.; Doyle, M. P.; McNamara, A. M.; Shefer, A. M.; Wells, J. G. Large outbreak of *E. coli* O157:H7 in western United States: The big picture. In *2nd International Symposium and Workshop on Verotoxin (Shiga-like Toxin) Producing E. coli Infections*; Goglio, M. A., Ed.; Elsevier: Amsterdam, 1994; pp 7–12.
- (4) Shere, J. A.; Bartlett, K. J.; Kaspar, C. W. Longitudinal study of *Escherichia coli* O157:H7 dissemination on four dairy farms in Wisconsin. *Appl. Environ. Microbiol.* **1998**, *64*, 1390–1399.
- (5) Bradford, S. A.; Schijven, J. Release of *Cryptosporidium* and *Giardia* from dairy calf manure: Impact of solution salinity. *Environ. Sci. Technol.* **2002**, *36*, 3916–3923.

- (6) Gagliardi, J. V.; Karns, J. S. Leaching of *Escherichia coli* O157:H7 in diverse soils under various agricultural management practices. *Appl. Environ. Microbiol.* **2000**, *66*, 877–883.
- (7) Himathongkham, S.; Riemann, H.; Bahari, S.; Nuanualsuwan, S.; Kass, P.; Oliver, D. O. Survival of *Salmonella typhimurium* and *Escherichia coli* O157:H7 in poultry manure and manure slurry at sublethal temperatures. *Avian Dis.* **2000**, *44*, 853–860.
- (8) Macler, B.; Merkle, J. Current knowledge on groundwater microbial pathogens and their control. *Hydrogeol. J.* **2000**, *8*, 29–40.
- (9) Craun, G. F.; Calderon, R. L.; Craun, M. F. *Waterborne Outbreaks Caused by Zoonotic Pathogens in the USA*; World Health Organization: Geneva, Switzerland, 2004.
- (10) CDC. *U. S. Questions & Answers: Sickness Caused by E. coli*; Centers for Disease Control and Prevention: Atlanta, GA, 2006; Vol. 2007.
- (11) Mead, P. S.; Slutsker, L.; Dietz, V.; McCaig, L. F.; Bresee, J. S.; Shapiro, C.; Griffin, P. M.; Tauxe, R. V. Food-related illness and death in the United States. *Emerging Infect. Dis.* **1999**, *5*, 607–625.
- (12) Pomeroy, B. S. *Fowl Typhoid*, 8th ed.; Iowa State University Press: Ames, IA, 1984.
- (13) Buxton, A.; Fraser, G. *Animal Microbiology*; Blackwell Scientific Publications: London, U.K., 1977; Vol. 1.
- (14) Ocholi, R. A.; Enurah, L. U.; Odeyemi, P. S. Fatal case of salmonellosis (*Salmonella pullorum*) in a chimpanzee (*Pan troglodytes*) in the Jos Zoo. *J. Wildl. Dis.* **1987**, *23*, 669–670.
- (15) Liu, G.-R.; Rahn, A.; Liu, W.-Q.; Sanderson, K. E.; Johnston, R. N.; Liu, S.-L. The evolving genome of *Salmonella enterica* serovar Pullorum. *J. Bacteriol.* **2002**, *184*, 2626–2633.
- (16) Pembrey, R. S.; Marshall, K. C.; Schneider, R. P. Cell surface analysis techniques: What do cell preparation protocols do to cell surface properties? *Appl. Environ. Microbiol.* **1999**, *65*, 2877–2894.
- (17) Shim, Y.; Lee, H. J.; Lee, S.; Moon, S. H.; Cho, J. Effects of natural organic matter and ionic species on membrane surface charge. *Environ. Sci. Technol.* **2002**, *36*, 3864–3871.
- (18) Walker, S. L.; Redman, J. A.; Elimelech, M. Influence of growth phase on bacterial deposition: Interaction mechanisms in packed-bed column and radial stagnation point flow systems. *Environ. Sci. Technol.* **2005**, *39*, 6405–6411.
- (19) Azeredo, J.; Lazarova, V.; Oliveira, R. Methods to extract the exopolymeric matrix from biofilms: A comparative study. *Water Sci. Technol.* **1999**, *39*, 243–250.
- (20) Switzer, R.; Garrity, L. *Experimental Biochemistry*; W. H. Freeman Publishing: New York, 1999.
- (21) Dubois, M.; Gilles, K. A.; Hamilton, J. K.; Rebers, P. A.; Smith, F. Colorimetric method for determination of sugars and related substances. *Anal. Chem.* **1956**, *28*, 350–356.
- (22) Elimelech, M.; Gregory, J.; Jia, X.; Williams, R. A. *Particle Deposition and Aggregation: Measurement, Modeling and Simulation*; Butterworth-Heinemann: Newton, MA, 1995.
- (23) Elimelech, M.; Nagai, M.; Ko, C. H.; Ryan, J. N. Relative insignificance of mineral grain zeta potential to colloid transport in geochemically heterogeneous porous media. *Environ. Sci. Technol.* **2000**, *34*, 2143–2148.
- (24) Walker, S. L.; Bhattacharjee, S.; Hoek, E. M. V.; Elimelech, M. A novel asymmetric clamping cell for measuring streaming potential of flat surfaces. *Langmuir* **2002**, *18*, 2193–2198.
- (25) Derjaguin, B. V.; Landau, L. Theory of the stability of strongly charged lyophobic sols and the adhesion of strongly charged particles in solutions of electrolytes. *Acta Physicochim. USSR* **1941**, *14*, 300.
- (26) Walker, S. L.; Redman, J. A.; Elimelech, M. Role of cell surface lipopolysaccharides in *Escherichia coli* K12 adhesion and transport. *Langmuir* **2004**, *20*, 7736–7746.
- (27) Bradford, S.; Simunek, J.; Walker, S. L. Transport and straining of *E. coli* O157:H7 in saturated porous media. *Water Resour. Res.* **2006**, *42*, W12S11–12.
- (28) Kretzschmar, R.; Borkovec, M.; Grolimund, D.; Elimelech, M. Mobile subsurface colloids and their role in contaminant transport. *Adv. Agron.* **1999**, *66*, 121–193.
- (29) Tufenkji, N.; Elimelech, M. Deviation from the classical colloid filtration theory in the presence of repulsive DLVO interactions. *Langmuir* **2004**, *20*, 10818–10828.
- (30) Lyklema, J. *Fundamentals of Interface and Colloid Science*; Academic Press: Amsterdam, The Netherlands, 1995; Vol. 2.
- (31) Camesano, T. A.; Logan, B. E. Influence of fluid velocity and cell concentration on the transport of motile and nonmotile bacteria in porous media. *Environ. Sci. Technol.* **1998**, *32*, 1699–1708.
- (32) Camesano, T. A.; Unice, K. M.; Logan, B. E. Blocking and ripening of colloids in porous media and their implications for bacterial transport. *Colloids Surf., A* **1999**, *160*, 291–308.
- (33) Dabroś, T.; van de Ven, T. G. M. Particle deposition on partially coated surfaces. *Colloids Surf., A* **1993**, *75*, 95–104.
- (34) Dabroś, T.; van de Ven, T. G. M. A direct method for studying particle deposition onto solid surfaces. *Colloid Polym. Sci.* **1983**, *261*, 694–707.
- (35) Rijnaarts, H. H. M.; Norde, W.; Bouwer, E. J.; Lyklema, J.; Zehnder, A. J. B. Bacterial deposition in porous media related to the clean bed collision efficiency and to substratum blocking by attached cells. *Environ. Sci. Technol.* **1996**, *30*, 2869–2876.
- (36) Meinders, J. M.; Noordmans, J.; Busscher, H. J. J. Simultaneous monitoring of the adsorption and desorption of colloidal particles during deposition in a parallel plate flow chamber. *Colloid Interface Sci.* **1992**, *152*, 265–280.
- (37) Meinders, J. M.; van der Mei, H. C.; Busscher, H. J. Deposition efficiency and reversibility of bacterial adhesion under flow. *J. Colloid Interface Sci.* **1995**, *176*, 329–341.
- (38) Meinders, J. M.; Vandermei, H. C.; Busscher, H. J. In situ enumeration of bacterial adhesion in a parallel plate flow chamber—elimination or in focus flowing bacteria from the analysis. *J. Microbiol. Methods* **1992**, *16*, 119–124.
- (39) Hahn, M. W.; O'Melia, C. R. Deposition and reentrainment of brownian particles in porous media under unfavorable chemical conditions: Some concepts and applications. *Environ. Sci. Technol.* **2004**, *38*, 210–220.
- (40) Albinger, O.; Biesemeyer, B. K.; Arnold, R. G.; Logan, B. E. Effect of bacterial heterogeneity on adhesion to uniform collectors by monoclonal populations. *FEMS Microbiol. Lett.* **1994**, *124*, 321–326.
- (41) Baygents, J. C.; Glynn, J. R.; Albinger, O.; Biesemeyer, B. K.; Ogden, K. L.; Arnold, R. G. Variation of surface charge density in monoclonal bacterial populations: Implications for transport through porous media. *Environ. Sci. Technol.* **1998**, *32*, 1596–1603.
- (42) Bolster, C. H.; Mills, A. L.; Hornberger, G.; Herman, J. Effect of intra-population variability on the long-distance transport of bacteria. *Ground Water* **2000**, *38*, 370–375.
- (43) Bradford, S. A.; Yates, S. R.; Bettahar, M.; Simunek, J. Physical factors affecting the transport and fate of colloids in saturated porous media. *Water Resour. Res.* **2002**, *38*, 1327–1339.
- (44) Bradford, S. A.; Bettahar, M. Straining, attachment, and detachment of *Cryptosporidium* oocysts in saturated porous media. *J. Environ. Qual.* **2005**, *34*, 469–478.
- (45) DeFlaun, M. F.; Murray, C. J.; Holben, W.; Scheibe, T.; Mills, A.; Ginn, T.; Griffin, T.; Majer, E.; Wilson, J. L. Preliminary observations on bacterial transport in a coastal plain aquifer. *FEMS Microbiol. Rev.* **1997**, *20*, 473–487.
- (46) Li, X. Q.; Scheibe, T. D.; Johnson, W. P. Apparent decreases in colloid deposition rate coefficients with distance of transport under unfavorable deposition conditions: A general phenomenon. *Environ. Sci. Technol.* **2004**, *38*, 5616–5625.
- (47) Redman, J. A.; Grant, S. B.; Olson, T. M.; Estes, M. K. Pathogen filtration, heterogeneity, and the potable reuse of wastewater. *Environ. Sci. Technol.* **2001**, *35*, 1798–1805.
- (48) Simoni, S. F.; Harms, H.; Bosma, T. N. P.; Zehnder, A. J. B. Population heterogeneity affects transport of bacteria through sand columns at low flow rates. *Environ. Sci. Technol.* **1998**, *32*, 2100–2105.
- (49) Zhang, X. Q.; Bishop, P. L. Spatial distribution of extracellular polymeric substances in biofilms. *J. Environ. Eng. (Reston, Va.)* **2001**, *127*, 850–856.
- (50) Tong, M.; Li, X.; Brow, C. N.; Johnson, W. P. Detachment-influenced transport of an adhesion-deficient bacterial strain within water-reactive porous media. *Environ. Sci. Technol.* **2005**, *39*, 2500–2508.
- (51) Liu, Y.; Schwartz, J.; Cavallaro, C. L. Catalytic dechlorination of polychlorinated biphenyls. *Environ. Sci. Technol.* **1995**, *29*, 836–840.
- (52) Tan, Y.; Gannon, J. T.; Baveye, P.; Alexander, M. Transport of bacteria in an aquifer sand—experiments and model simulations. *Water Resour. Res.* **1995**, *31*, 2381–2381.
- (53) Tufenkji, N.; Redman, J. A.; Elimelech, M. Interpreting deposition patterns of microbial particles in laboratory-scale column experiments. *Environ. Sci. Technol.* **2003**, *37*, 616–623.
- (54) Kim, H. N.; Walker, S. L. *Escherichia coli* transport in porous media: Influence of cell strain, solution chemistry, and temperature. *Colloids Surf., A*, submitted for publication.

- (55) Torkzaban, S.; Tazehkand, S. S.; Bradford, S. A.; Walker, S. L. Transport and fate of bacteria in porous media: Coupled effects of chemical conditions and pore space geometry. *Water Resour. Res.* **2008**, *44*, W04403, doi: 10.1029/2007WR006541.
- (56) Kretzschmar, R.; Barmettler, K.; Grolimun, D.; Yan, Y. D.; Borkovec, M.; Sticher, H. Experimental determination of colloid deposition rates and collision efficiencies in natural porous media. *Water Resour. Res.* **1997**, *33*, 1129–1138.
- (57) Li, X.; Zhang, P.; Lin, C. L.; Johnson, W. P. Role of hydrodynamic drag on microsphere deposition and re-entrainment in porous media under unfavorable conditions. *Environ. Sci. Technol.* **2005**, *39*, 4012–4020.
- (58) Redman, J. A.; Walker, S. L.; Elimelech, M. Bacterial adhesion and transport in porous media: Role of the secondary energy minimum. *Environ. Sci. Technol.* **2004**, *38*, 1777–1785.
- (59) O'Melia, C. R. *Kinetics of Colloidal Chemical Processes in Aquatic Systems*; Wiley Interscience: New York, 1990.
- (60) Yao, K. M.; Habibian, M. T.; O'Melia, C. R. Water and waste water filtration: Concepts and applications. *Environ. Sci. Technol.* **1971**, *5*, 1105–1112.
- (61) Rajagopalan, R.; Tien, C. Trajectory analysis of deep-bed filtration with the sphere-in-cell porous media model. *AIChE J.* **1976**, *22*, 523–533.
- (62) Liu, Y.; Yang, C. H.; Li, J. Adhesion and retention of a bacterial phytopathogen *Erwinia chrysanthemi* in biofilm-coated porous media. *Environ. Sci. Technol.* **2008**, *42*, 159–165.
- (63) Cunningham, A. B.; Sharp, R. R.; Caccavo, F.; Gerlach, R. Effects of starvation on bacterial transport through porous media. *Adv. Water Res.* **2007**, *30*, 1583–1592.

ES802531K